Microwave Noise Characterization of GaAs MESFET's: Evaluation by On-Wafer Low-Frequency Output Noise Current Measurement

MADHU S. GUPTA, SENIOR MEMBER, IEEE, OCTAVIUS PITZALIS, JR., MEMBER, IEEE, STEVEN E. ROSENBAUM, MEMBER, IEEE, AND PAUL T. GREILING, FELLOW, IEEE

Abstract — A simplified noise equivalent circuit is presented for submicron-gate-length MESFET's in the common-source configuration, consisting of five linear circuit elements: the gate-to source capacitance C_{gs}, the total input resistance R_T, the transconductance g_m, the output resistance R_o, and a noise current source of spectral density S_{io} at the output port. All of these elements can be determined by on-wafer measurements, and the noise current can be measured at a low frequency. The minimum noise figure of the device calculated from this model, as well as the bias and frequency dependence of the noise figure, is shown to be in agreement with microwave noise figure measurements. Thus a technique has been established for determination of the minimum noise figure of a device solely by on-wafer measurements rather than by the usual microwave measurements. The proposed technique can be employed rapidly, conveniently, without the need for tuning, and at the wafer stage of device fabrication.

I. Introduction

A. Motivation

THE GaAs MESFET's are well established as the principal low-noise active devices in the microwave and millimeter-wave frequency range. In addition to their other advantages, such as versatility of applications, suitability for monolithic integration, high dc-to-RF conversion efficiency, high input–output isolation, and wide frequency range of applicability, the MESFET's (as well as the HEMT's) have the lowest noise among all present three-terminal active devices. Under cyrogenic conditions, their noise figure closely approaches that of masers [1]. The widespread use of these devices in low-noise applications accounts for the strong interest in methods of determining and predicting their noise figure in an efficient manner.

The presently available methods for determining the noise figure of MESFET's are adequate for laboratory work, but inconvenient in a production setting. The experimental measurement of the noise figure requires mounting the device in a microwave fixture, tuning of the circuit, and optimizing generator admittance;[1] even with an automatic noise figure meter it is a time-consuming procedure, leading to the search for improved methods [2], [3]. The calculation of the noise figure based on theoretical noise models [4], [5] requires a knowledge of a large number of theoretical parameters which are not known for devices in production, and which would require even more effort to determine. Empirical models for calculating the noise figure, on the other hand, require a knowledge of some empirical fitting parameters [6]–[9], which will vary from device to device, and which can be found for a given lot of devices only after their noise figure has already been determined. Clearly, there is a need to develop methods for rapidly and efficiently determining the noise performance of these devices. The present paper addresses this need.

B. The Problem

The noise figure F of a MESFET is an important device specification, and in some applications it is the principal performance parameter, overriding other device requirements. The MESFET's produced for such applications must be tested to verify that they meet the noise figure requirement at the desired frequency of operation f_o. Since f_o can be a microwave or a millimeter-wave frequency, this testing is traditionally carried out in a microwave measurement setup which requires manual tuning by a trial-and-error method and which accepts a single device at a time, typically mounted and bonded on a carrier. Such testing is very expensive in a production setting for two reasons:

(i) Since the devices have already been mounted and bonded, they must be individually handled in the testing procedure, unlike the testing at the wafer stage prior to dicing, when all devices could be tested with only one wafer-handling operation.

Manuscript received April 6, 1987; revised August 17, 1987.

M. S Gupta is with the Department of Electrical Engineering and Computer Science, University of Illinois at Chicago, Chicago, IL 60680.
O. Pitzalis, Jr., was with Hughes Research Laboratories, Malibu, CA. He is now with EEsof, Inc., Westlake Village, CA 91362.
S. E. Rosenbaum and P. T. Greiling are with Hughes Research Laboratories, Malibu, CA 90265.

IEEE Log Number 8717496.

[1] The term "generator" is used in place of the more common term "source" throughout this paper to avoid confusion with the MESFET terminal called "source."

0018-9480/87/1200-1208$01.00 ©1987 IEEE

(ii) Since the yield of high-performance devices is low (particularly for mm-wave devices, which have such small dimensions that their characteristics change significantly with the etching of even several atomic layers during fabrication), the individual mounting, bonding, and testing steps carried out on rejected devices are wasted.

It is clear that an ability to test at the wafer stage for noise figure of the device at f_o can result in substantial cost savings. There are several obstacles to achieving this desirable goal by the conventional method of noise figure measurement:

(i) In state-of-the-art testing equipment, capable of handling entire wafers, the probes used for accessing the individual devices contribute parasitic impedances, which can be made tolerable at UHF and low microwave frequencies. However at the high end of the microwave frequency range, the probes have a significant, or even dominant, effect on the value of the generator admittance Y_g presented to the device during the measurement of the noise figure at f_o, and hence on the measured value of F.

(ii) The minimum noise figure F_{min} can either be determined by actual variation of Y_g to minimize the measured F or be deduced from the data if four or more values of F are measured for four well-separated values of Y_g. In either case, the tuning of Y_g over a wide range, and the measurement of the generator admittances Y_g actually presented to the device, are difficult in a probe station setup at high microwave frequencies.

(iii) The above-mentioned problems of determining F_{min} (as well as the other three noise parameters) can be ameliorated if the noise figure F is measured at a sufficiently low frequency f_L (e.g., at a UHF or L-band frequency), where the probe station parasitics are small. In this case, a method must be devised for predicting the F_{min} of the device at f_o from the data at f_L. Experimental measurements of the noise figure of mm-wave MESFET devices as a function of frequency have shown that at low frequency (typically below a few GHz for 0.25-μm-gate devices), the measured noise figure is strongly influenced by the circuit losses. (This point is clarified in Section II-E of this paper, where it is shown that F_{min} at f_L and at f_o is given by two different expressions, equations (15) and (17), respectively.) As a result, the measured F_{min} at f_L is not a direct measure of the device capability at f_o, and cannot be used to predict the high-frequency device performance. Attempts to reduce circuit losses at f_L are again stymied by the wafer-handling probe station.

This paper presents an alternate solution to the problem of predicting $F_{min}(f_o)$ on the basis of measurements which can be carried out on an automated wafer probe station and which involve only a low-frequency noise measurement.

C. Outline

The method presented is based on a highly simplified noise equivalent circuit model of the MESFET, containing only four lumped circuit elements and one noise current source. Each of these five model elements is dependent on the dc bias of the device, but not on f_o. The validity of such a simplified model is established experimentally. This paper presents a description and verification of the noise model, and of its use for predicting $F_{min}(f_o)$, in three steps:

(i) In Section II, the noise figure of a MESFET amplifier is calculated starting from a general noise model, employing two partially correlated noise sources, and then a simplification of the model is introduced.

(ii) In Section III brief details of the MESFET's on which experiments were performed are summarized; the on-wafer methods of measurement are described; and the results obtained from those measurements on the devices under test are given.

(iii) In Section IV, the microwave noise performance of the MESFET's, determined by actual RF measurements at f_o, is compared with predictions based on the noise model and the on-wafer measurements.

II. Calculation of Noise Figure

This section contains details of the MESFET noise equivalent circuit model, the calculation of amplifier noise figure, and the simplification of the model under suitable assumptions.

A. Factors Influencing the Noise Figure

To understand the scope and method of this paper, it is helpful to list all those factors whose influence on the noise figure F of a MESFET microwave amplifier is correctly predicted by the model proposed in this paper. The numerous other design variables that influence F, including the device material, design, and dimensions and the choice of RF circuit design, will be treated as invariants. In particular, the circuit will be assumed to be a single common-source stage without feedback, which has the advantages of simplicity of circuit design and ease of performance calculation.

In this configuration, the noise figure depends on six parameters: the three parameters describing the circuit (the frequency of interest f_o and the generator conductance G_g and susceptance B_g at this frequency) and the three parameters describing the operating point of the device (the temperature T, the dc drain-to-source voltage V_{DS}, and the dc drain current I_D of the MESFET). The dependence of F on these six variables is known [10] from theoretical models, experimental measurements, and empirical formulas, and is illustrated in Fig. 1 for a typical submicron-gate MESFET. In particular, the temperature dependence has been studied in detail elsewhere [11], and the present paper will assume room-temperature device operation. The influence of the remaining five parameters on F is central to the present paper, and is briefly summarized below.

(*i*) *The generator admittance* $Y_g = G_g + jB_g$, connected at the input port of the amplifier, influences the amplifier F in a manner which is precisely known [12] for any linear

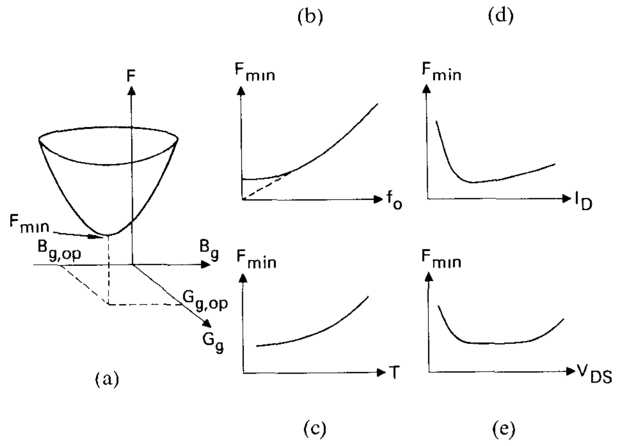

Fig. 1. Factors influencing the noise figure of a typical submicron-gate-length MESFET amplifier. (a) Generator admittance $G_g + jB_g$. (b) Operating frequency f_o. (c) Temperature T. (d) dc drain current I_D. (e) dc drain-to-source voltage V_{DS}.

two-port:

$$F(Y_g) = F_{\min} + \frac{R_n}{G_g}\left[\left(G_g - G_{g,\mathrm{op}}\right)^2 + \left(B_g - B_{g,\mathrm{op}}\right)^2\right] \quad (1)$$

where

$F_{\min}$ = the minimum value of $F(Y_g)$, minimized with respect to Y_g;

$Y_{g,\mathrm{op}}$ = $G_{g,\mathrm{op}} + jB_{g,\mathrm{op}}$, the optimum value of Y_g for which $F(Y_g)$ attains the value $F_{\min}$;

R_n = a quantity, having the units of resistance, which is a measure of the sensitivity of $F(Y_g)$ to deviations of Y_g from its optimum value $Y_{g,\mathrm{op}}$.

The dependence of $F(Y_g)$ on Y_g is illustrated in Fig. 1(a).

Since the variation of the device operating conditions (f_o, I_D, and V_{DS}) can cause a change in $F(Y_g)$ both directly as well as indirectly via $Y_{g,\mathrm{op}}$, whereas $F_{\min}$ is a characteristic of the device unaffected by changes in $Y_{g,\mathrm{op}}$, the following discussion describes the influence of these operating conditions on $F_{\min}$ rather than on F.

(*ii*) *The operating frequency f_o* influences $F_{\min}$ as shown by the dotted curve in Fig. 1(b). The monotonic decrease of $F_{\min}$ towards unity ($= 0$ dB) as f_o decreases is due to the decrease of input conductance of the device with decreasing frequency. This effect has been predicted theoretically [4], and is implicit in many empirical formulas for $F_{\min}$ [6]–[9]. Experimental measurements, on the other hand, determine $F_{\min}$ of an amplifier circuit rather than of the intrinsic device, and its observed variation with frequency is shown by the solid line in Fig. 1(b). At low frequencies, where the circuit losses dominate at the input port, the circuit $F_{\min}$ approaches a constant value (> 0 dB), which depends on the circuit losses.

(*iii*) *The dc drain current I_D* influences $F_{\min}$ in the manner shown in Fig. 1(d), with the noise figure attaining a minimum for a drain current equal to a fraction (typically a third to a sixth) of I_{DSS}, the saturated value of I_D for zero gate bias. The noise figure increases very rapidly below the optimum bias current, but only slowly above it, as shown in Fig. 1(d). This effect has been predicted both from theoretical considerations [4] and is observed in experimental measurements [13]. The minimum in $F_{\min}$ arises because at low values of I_D, the device transconductance g_m is smaller while at high values of I_D the noise generation is larger, and either condition increases $F_{\min}$.

(*iv*) *The drain voltage V_{DS}* has little influence on $F_{\min}$, provided the MESFET is biased in the current saturation region. In the linear region (where V_{DS} is below the "knee" in the I_D–V_{DS} characteristic), the noise figure will be larger due to lower device gain. At large V_{DS} the noise figure again increases due to a number of reasons, including increase in I_D, possible Gunn domain formation, and avalanching in the channel [14].

From the foregoing discussion, it is apparent that a noise model of MESFET device will be useful only if it correctly predicts $F_{\min}$ as a function of I_D, V_{DS}, and f_o. This criterion will be used in Section IV to validate the proposed noise model.

B. RF Model of Device and Amplifier

Numerous equivalent circuit models of MESFET's have been reported differing from each other in their frequency range of applicability, inclusion of nonlinearities, accounting of device parasitics, etc. Since our goal is only to predict the noise performance of devices which are still in the wafer stage of fabrication, and since the important performance measures such as $F_{\min}$ and maximum available gain are invariant with respect to lossless transformations at the input and output ports, the inclusion of most parasitics is unnecessary for present purposes, and a simple model will suffice. All MESFET models must include the two essential intrinsic elements of the device: the input gate-to-source capacitance C_{gs} and a controlled current source at the output port. Since a model with only these two elements would have an unlimited frequency response and available output power, at least two additional elements must be added to it: the total input resistance R_T in series with C_{gs}, and the output resistance R_o in parallel with the current source. These four elements constitute the simplest possible equivalent circuit that is adequate for the present purposes, and is shown in the dotted box labeled "device" in Fig. 2(a). All of the four circuit elements in this model are linear, dc bias dependent, and independent of frequency.

Since the net Y_g connected at the input port of the device is a crucial quantity in determining and minimizing the noise figure, a more realistic model may include the bonding wire inductance L_w shown dotted in Fig. 2(a). Indeed, in many measurement techniques, the reference plane at which Y_g and device parameters are measured is so defined that L_w is treated as a part of the device. Since the purpose of this paper is only to predict $F_{\min}$, which is not influenced by lossless parasitic elements, L_w can be set equal to zero. The lossless parasitic elements will become significant in a sequel to this paper [15], where other noise parameters are also of interest.

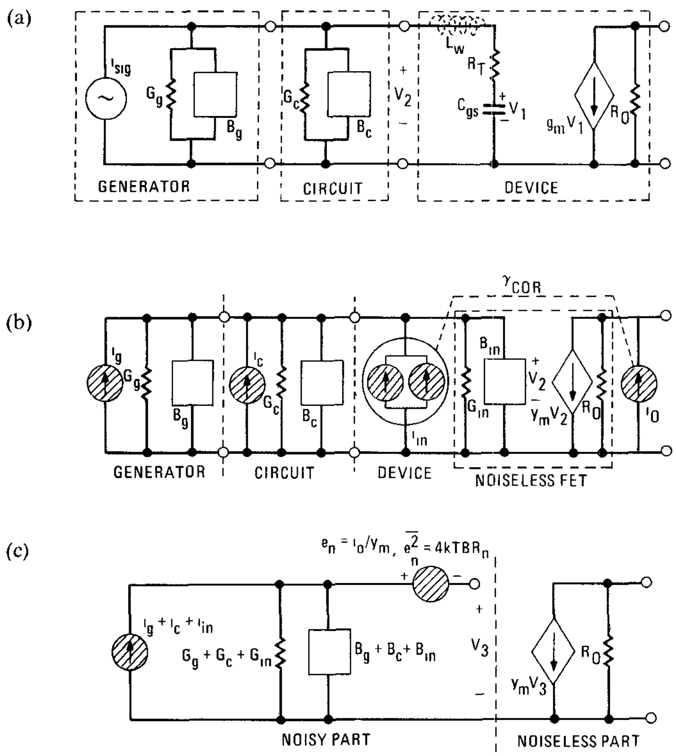

Fig. 2. Circuit models used in the calculation of the noise parameters of the MESFET amplifier. (a) Idealized linear amplifier circuit. (b) Noise equivalent circuit of the amplifier. (c) Simplified noise equivalent circuit.

Experimental measurements do not yield the noise figure of a device, but only that of a circuit in which the device is embedded. In general, the measured noise figure will not be a characteristic of the device alone, but will also depend on the embedding circuit [16]. Therefore a circuit model of the amplifier is also needed for calculation of a noise figure that can be compared with measurements. Once again, the simplest possible circuit has been selected for our analysis. This circuit is schematically shown in Fig. 2(a), and consists of a single circuit admittance Y_c interposed between the generator and the active device.

C. Noise Equivalent Circuit

The noise equivalent circuit of the amplifier of Fig. 2(a), required for the calculation of noise figure, is shown in Fig. 2(b). In this noise model, the thermal noise generated in G_g and G_c is represented by noise current sources i_g and i_c, respectively, whose power spectral densities are obtained from the noise temperatures of the two conductances using Nyquist's theorem. Since the goal is to calculate the noise figure, the noise temperature of G_g will be taken to be the reference temperature T_{ref} ($=290$ K) to conform with the IRE definition of noise figure [17]. The noise temperature of G_c is the ambient temperature at which the circuit is maintained, and is assumed to be the same as T_{ref} for simplicity; our calculations will therefore require a small modification if, for example, the amplifier is cryogenically cooled.

The noise in the active device is modeled by the two noise current sources i_{in} and i_o connected in shunt with the input and the output ports of the noiseless linear (small-signal) circuit model of the device, as shown in Fig. 2(b). The principal advantage of this device noise model, compared to the other possible representations [12], is that the two noise sources i_{in} and i_o can be directly identified with gate and drain noise currents, respectively. The input noise source i_{in} can be subdivided into two parts: one uncorrelated and the other completely correlated with the output noise source i_o.

One other modification has been introduced in Fig. 2(b). The dependent current source $g_m V_1$ is written as $y_m V_2$, controlled by the voltage V_2, defined across the entire input admittance $(G_{in} + jB_{in})$ of the device, instead of V_1, which was only across C_{gs}. The transconductance g_m is thus replaced by a transadmittance

$$y_m = (V_1/V_2) g_m \tag{2}$$

where

$$V_2 = (1 + j\omega C_{gs} R_T) V_1. \tag{3}$$

D. Calculation of Noise Figure

The noise equivalent circuit of Fig. 2(b) can be configured as in Fig. 2(c), where the mutually uncorrelated noise sources i_g, i_c, and i_{in} are combined, as are also the admittances $G_g + jB_g$, $G_c + jB_c$, and $G_{in} + jB_{in}$. In addition, the noise current source i_o at the output port is replaced by an equivalent noise voltage source e_n on the input side which is fully correlated with i_o, and which is added to the controlling voltage V_2. The source e_n is related to i_o by a correlation admittance equal to y_m; i.e., their correlation coefficient is $y_m/|y_m|$, and their spectral densities S_{en} and S_{io} are related by

$$S_{io}(\omega) = |y_m|^2 S_{en}(\omega). \tag{4}$$

Three new parameters are now defined so as to express the results more compactly.

(i) An "equivalent noise resistance" $R_n(\omega)$ is defined as that resistance which, when maintained at the reference temperature T_{ref} of 290 K, will produce an open-circuit noise voltage having the same spectral density as $S_{en}(\omega)$. From (2), (3), and (4),

$$R_n(\omega) \equiv S_{en}(\omega)/4kT_{\text{ref}} = \frac{S_{io}(\omega)/4kT_{\text{ref}}}{g_m^2/\left(1+\omega^2 C_{gs}^2 R_T^2\right)} \tag{5}$$

where k is Boltzmann's constant.

(ii) An "uncorrelated noise conductance" G_{un} is similarly defined as the conductance which, when kept at T_{ref}, will produce a short-circuit thermal noise current having the same spectrum as the spectrum of the uncorrelated part of i_{in}.

(iii) A correlation admittance Y_{cor} is defined as the transfer function relating the noise voltage e_n to that part of the noise current i_{in} which is fully correlated with i_o.

The noise figure of the amplifier circuit at a spot frequency then follows from the definition as

$$F(Y_g) \equiv \frac{\langle V_3^2 \rangle}{\langle V_3^2 \rangle \text{ with } i_c = i_{in} = e_n = 0}$$
$$= 1 + \frac{G_c + G_{\text{un}}}{G_g} + \frac{R_m}{G_g}\left(|Y_g + Y_c + Y_{in} + Y_{\text{cor}}|^2\right) \quad (6)$$

where $\langle \cdot \rangle$ denotes the average value in a narrow bandwidth at the spot frequency. The four noise parameters $G_{g,\text{op}}$, $B_{g,\text{op}}$, F_{min}, and R_n of the amplifier can be deduced from this expression. The noise figure becomes a minimum for a generator admittance

$$Y_{g,\text{op}} \equiv G_{g,\text{op}} + jB_{g,\text{op}}$$
$$= \left[(G_c + G_{in} + G_{\text{cor}})^2 + \frac{G_c + G_{\text{un}}}{R_m}\right]^{1/2}$$
$$- j[B_c + B_{in} + B_{\text{cor}}] \quad (7)$$

and attains the minimum value of

$$F_{\text{min}} = 1 + \frac{R_m}{G_{\text{op}}}\left[2G_{g,\text{op}}^2 + 2G_{g,\text{op}}(G_c + G_{in} + G_{\text{cor}})\right]$$
$$= 1 + 2R_m(G_c + G_{in} + G_{\text{cor}})$$
$$+ 2\sqrt{R_m(G_c + G_{\text{un}}) + R_m^2(G_c + G_{in} + G_{\text{cor}})^2}. \quad (8)$$

The fourth noise parameter R_n can be found by rewriting (6) in terms of $Y_{g,\text{op}}$ and F_{min}, as in (1), leading to the result

$$R_n = R_m. \quad (9)$$

E. Simplifications

In general, the calculated F_{min} is influenced by both noise sources i_{in} and i_o. Considerable economy in the measurement and characterization procedures results if the effect of one of these sources (namely i_{in}, which is the smaller of the two) is accounted for without a direct measurement of that source. With this objective in mind, consider the various mechanisms contributing to i_{in}. The part of i_{in} which is correlated with i_o arises predominantly from the noise current induced in the gate by the noise in the channel current. Since the coupling between the gate and the channel is primarily capacitive, the complex correlation coefficient γ_{cor} between i_{in} and i_o is mostly imaginary with only a small real part. The uncorrelated part of i_{in} arises from thermal noise in the input conductance G_{in} of the device, the noise in gate leakage current, and the induced gate noise current.

Two assumptions will now be introduced which simplify the determination of F_{min} by allowing the effect of each of the above two parts of i_{in} to be estimated, without their explicit measurement.

(i) Moderate Frequency Assumption: If the operating frequency f_o is significantly below the device cutoff frequency f_t, the following approximation holds:

$$\omega_o^2 C_{gs}^2 R_T^2 \ll 1. \quad (10)$$

Under this condition, the transadmittance y_m in (2) is purely real, so that the correlation coefficient between i_{in} and e_n, like that between i_{in} and i_o, is largely imaginary, i.e.,

$$G_{\text{cor}} \simeq 0. \quad (11)$$

Then F_{min} in (8) is not influenced by the correlation between i_{in} and i_o, even if the two sources are highly correlated.

(ii) Low Leakage Assumption: In good low-noise MESFET's, the gate leakage current is small under normal operating conditions, so that the corresponding shot noise is negligible. Furthermore, the uncorrelated part of the induced gate noise current, which varies as ω^2, is small if the frequencies are restricted to low and moderate values in accordance with (10). Under these conditions, the uncorrelated part of i_{in} is dominated by the thermal noise in the input conductance G_{in}. The thermal noise in G_{in} comes from two sources: the thermal noise of resistances which contribute also to i_o (and therefore to the correlated part of i_{in}), and the thermal noise of resistances contributing to the uncorrelated part of i_{in}. Since the former resistances are small compared to the latter, the entire thermal noise of G_{in} may be identified with the uncorrelated part of i_{in}. Since the device has been assumed to be at the reference temperature T_{ref}, it follows from the definition of the "uncorrelated noise conductance" in Section II-D that

$$G_{\text{un}} \simeq G_{in}. \quad (12)$$

With the above two assumptions, the noise figure in (8) reduces to

$$F_{\text{min}} = 1 + 2R_n(G_c + G_{in})$$
$$+ 2\sqrt{R_n(G_c + G_{in}) + R_n^2(G_c + G_{in})^2}. \quad (13)$$

Two limiting values of this expression are of interest:

(i) Low Frequency Limit: Since the input conductance of the device,

$$G_{in} = \frac{\omega^2 C_{gs}^2 R_T}{1 + \omega^2 C_{gs}^2 R_T^2} \quad (14)$$

vanishes at low frequencies, F_{min} at low frequencies approaches the limiting value

$$F_{\text{min}} = 1 + 2R_n G_c + 2\sqrt{R_n G_c + R_n^2 G_c^2} \qquad \text{for } G_{in} \ll G_c \quad (15)$$

which is dependent on the circuit losses.

(ii) Low Circuit-Loss Limit: Conversely, if the circuit losses are negligible or at frequencies sufficiently high that G_c can be neglected compared to G_{in},

$$G_c \ll G_{in} \quad (16)$$

the F_{min} in (13) becomes

$$F_{\text{min}} = 1 + 2R_n G_{in} + 2\sqrt{R_n G_{in} + R_n^2 G_{in}^2} \qquad \text{for } G_c \ll G_{in}. \quad (17)$$

This quantity is a characteristic of the device, independent of the circuit, and approaches 0 dB at low frequencies, since G_{in} vanishes there provided the assumption (16) continues to hold. Since this quantity is independent of circuit parameters and is a characteristic of the device, it can be called the "device noise figure." The expression in (17) is identical with the expression used by Bruncke and van der Ziel [18] and by Podell [8]. The assumptions implicit in the empirical MESFET noise model of Podell [8] are thus clarified.

III. The On-Wafer Device and Noise Parameter Measurements

This section presents the on-wafer measurement methods used for measuring the values of the parameters C_{gs}, R_T, g_m, R_o, and S_{io} appearing in the device model, for a given device and under given dc bias conditions. The measurements are made with the wafer placed on a micromanipulator station, and contacted by micro probes leading to coaxial lines having a characteristic impedance of 50 Ω, similar to those described in the literature [19]. The experimental results obtained are also presented, and are used for model validation in the next section.

A. The GaAs MESFET Device

All experimental data reported in this paper were obtained on GaAs MESFET's which are state-of-the-art devices under development. They have a gate electrode of T cross section for reduced gate resistance, with a gate length of 0.2 μm and a gate width of 75 μm. The Schottky-barrier gate junction is made with Ti/Pt/Au on an active layer grown by vapor phase epitaxy. The pinchoff voltage of the devices (defined at $V_{DS} = 3$ V, and $I_D = 0.1$ mA) is approximately −2.1 V. The dc characteristics of these devices are shown in Fig. 3.

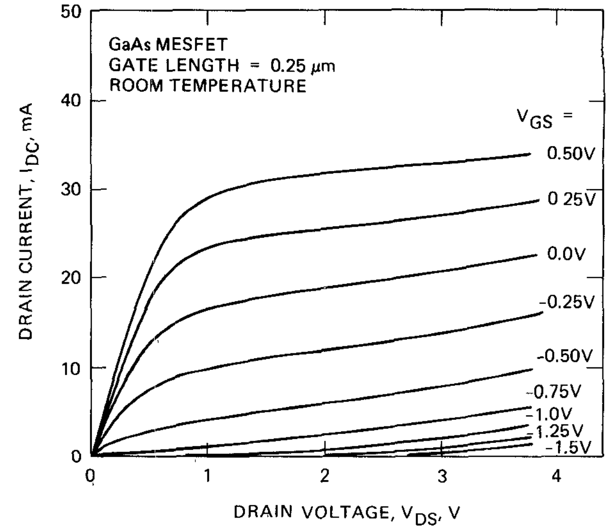

Fig. 3. dc current–voltage characteristics of the low-noise MESFET employed in this paper.

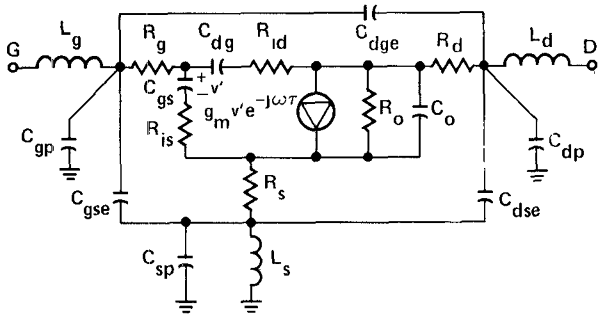

Fig. 4. Small-signal model of the FET in common-source configuration, used for fitting to the measured S parameters. The parameters C_{gs}, g_m, and R_o are defined in the text. L_g, L_s, and L_d are bond-wire inductances; C_{gp}, C_{sp}, and C_{dp} are the bonding pad capacitances; C_{gse}, C_{dge}, and C_{dse} are the extrinsic interelectrode capacitances; R_g, R_s, and R_d are the series parasitic resistances; R_{is} is the effective channel resistance; C_o is the output drain-to-source capacitance; R_{id} and C_{dg} are the gate-to-drain feedback resistance and capacitance, with C_{dg} typically an order of magnitude smaller than C_{gs}; and τ accounts for the phase delay in drain current with reference to the controlling voltage v'.

B. On-Wafer Measurement of Signal Parameters

Under a given set of dc bias conditions, the four device parameters g_m, C_{gs}, R_T, and R_o are measured as follows. A small-signal model for the MESFET device, having frequency-independent elements and incorporating pad and bond wire parasitics is shown in Fig. 4. It is an accurate representation of the device over a wide frequency range (≈ dc to 40 GHz). The MESFET under test was characterized over the frequency range 45 MHz to 18 GHz by S-parameter measurements, and then a computer program was used to determine the values of the equivalent circuit parameters appearing in Fig. 4 for a least-mean-square-error fit to the measured S parameters. The four device model parameters of Fig. 2(a) were calculated from the fitted parameters of Fig. 4 for each bias value as follows:

(i) The total input resistance, $R_T = R_g + R_{is} + R_s$.

(ii) The input capacitance C_{gs} is equal to the intrinsic gate-to-source capacitance C_{gs} of Fig. 4.

(iii) The transconductance g_m is identical in the two models.

(iv) The output resistance R_o is also identical in the two models since R_d is much smaller than R_o.

This procedure was repeated at each dc bias condition of interest to find the bias dependence of each element. These four parameters are shown plotted as a function of dc drain current I_D, and for a fixed drain-to-source voltage $V_{DS} = 3$ V, in Fig. 5. The values of g_m and C_{gs} obtained in this manner show excellent agreement with the results of low-frequency and bridge measurements. This is taken to be an independent validation of the on-wafer method of obtaining these parameters.

C. Output Noise Current Measurement

For MESFET's in common-source configuration, the power spectral density S_{io} of the short-circuit noise current i_o at the output port can be measured directly with a low-noise receiver, as indicated in Fig. 6. In low noise MESFET's, S_{io} is frequency-independent in the microwave frequency range [20], so that its measurement can be carried out at a convenient low frequency f_L. The receiver measures the noise power P_{out} delivered by the device to the input resistance R_r of the narrow-band receiver in an

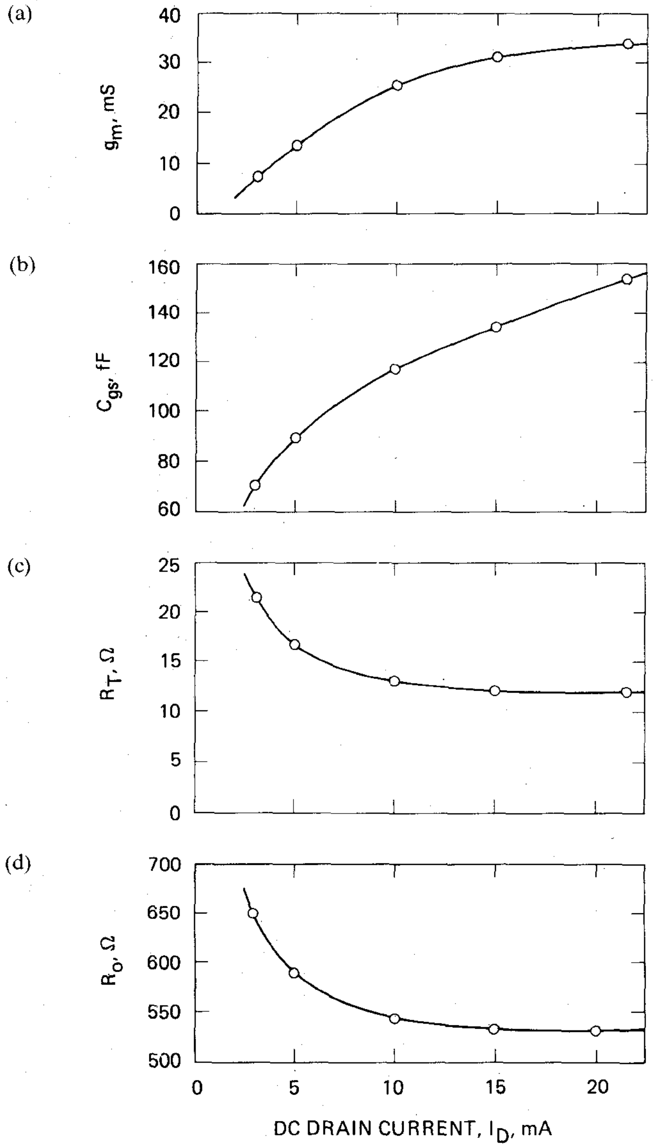

Fig. 5. Measured equivalent-circuit parameters at a fixed dc drain-to-source voltage $V_{DS} = 3$ V. (a) Transconductance g_m. (b) Gate-to-source capacitance C_{gs}. (c) Total input resistance $R_T = R_g + R_i + R_s$. (d) Output resistance R_o.

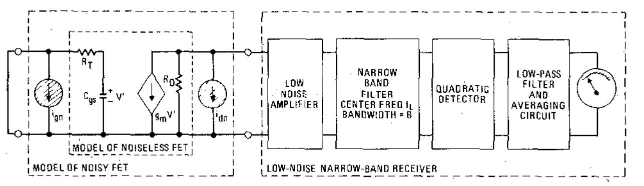

Fig. 6. Experimental setup for measuring the noise power output of the device at frequency f_L in a bandwidth B. Input resistance of the receiver is R_r.

effective noise bandwidth B at the frequency f_L of measurement, from which $S_{io}(f_o)$ is calculated:

$$S_{io}(f_o) \simeq S_{io}(f_L) = \frac{P_{\text{out}}}{B} \frac{(R_r + R_o)^2}{R_o^2 R_r}. \tag{18}$$

The following remarks concerning this measurement are

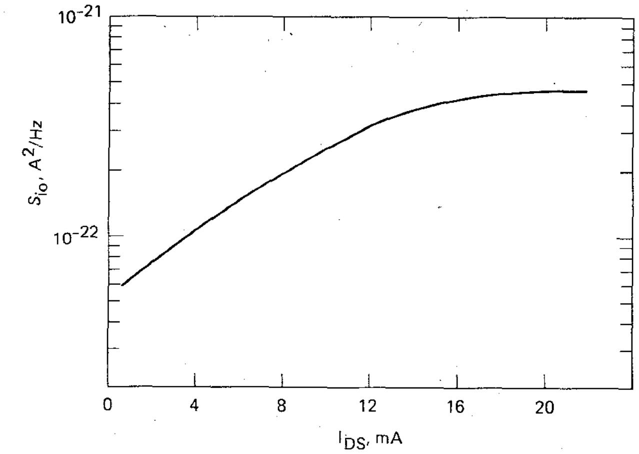

Fig. 7. Measured spectral density of the short-circuit noise current at the output port of the device, with the input port short-circuited, and at $V_{DS} = 3$ V.

relevant:

(i) The measurement frequency f_L should be sufficiently high that the effects of low-frequency noise sources, such as $1/f$ and generation–recombination noise, are negligible at f_L, thus ensuring that S_{io} is flat between f_L and f_o. At the same time, it is convenient if f_L is low enough that low-noise amplifiers are available. These considerations would dictate a frequency somewhere in the tens of MHz to a few GHz. Our own measurements from 30 MHz to 1.2 GHz showed that the power spectral density was constant, and the exact frequency of measurement in this range was immaterial.

(ii) The RF short circuit required at the gate–source port is easier to provide at the low measurement frequency f_L than at a microwave frequency. In our measurements, this was done by a dc-blocking capacitor right at the probes used in the on-wafer measurements to contact the device terminals. No instabilities resulted by this procedure for the devices tested.

(iii) In practice, the low-noise receiver can be a communication receiver or a spectrum analyzer, preceded by a preamplifier of sufficiently low noise and high gain. In order to determine the gain and noise figure requirements for this preamplifier, the noise level to be measured can be estimated by using the approximate rule of thumb [21] that the effective noise temperature at the output port of the device is of the order of $g_m R_o$ times the physical temperature of the device.

(iv) The only use made of the measured value of the model parameter R_o is in calculating S_{io} from (18). For many commercially available low-noise preamplifiers, the input impedance R_r is nominally 50 Ω, while R_o (for devices with 75 µm gate width) is usually an order of magnitude larger under typical dc bias conditions. Thus R_o may be ignored in calculating S_{io}, and the measurement of R_o can be entirely omitted.

(v) In order to determine S_{io} in absolute units (A^2/Hz), the effective noise bandwidth B of the receiver must be accurately known or measured. For sufficiently low noise preamplifiers, B can be found by measuring the thermal noise at the output port of the device with zero gate and drain bias, and employing Nyquist's theorem which applies to the device in thermal equilibrium.

The power spectrum of output noise current was measured in this manner, as a function of f_L, I_D, and V_{DS}, and the results are shown in Fig. 7 for one of the tested MESFET's. Over the frequency range of 30 MHz to 1.2 GHz, and for V_{DS} in the range 1 V to 4 V, S_{io} was constant and was dependent only on I_D, as shown in Fig. 7.

IV. Predicted and Measured Noise Performance

In this section, the minimum noise figure of the device, measured at microwave frequencies, is compared with the F_{min} predicted by the device noise model, using the parameter values obtained from on-wafer measurements.

A. Noise Figure Performance

The noise figure of the MESFET amplifier has been expressed in (13) in terms of the three quantities R_n, G_{in}, and G_c. The first two of these can be calculated from (5) and (14), using the values of C_{gs}, R_T, g_m, and S_{io}, obtained from on-wafer measurements. The third quantity G_c depends on the embedding circuit in which the MESFET noise figure is to be determined, and it can be estimated as follows. If the insertion loss of the "front half" of the amplifier circuit (i.e., the part between the generator and the gate port) is measured in a matched system of characteristic impedance R_{ref} (which will typically be 50 Ω) and is found to be small, it can be expressed approximately as

$$L_{ins} = 1 + R_{ref} G_c. \tag{19}$$

Thus a measurement of insertion loss yields G_c. The measured insertion loss, although dependent on the circuit construction and connectors used, was found to be approximately independent of frequency at lower frequencies (below 10 GHz). At higher frequencies, G_c has only a very small effect on F_{min}, since it is masked by G_{min}, and therefore its exact value is not required. Therefore, G_c can be treated as a frequency-independent parameter. The value of G_c estimated in this manner was further verified as follows. The minimum noise figure of the amplifier at low frequencies is frequency-independent, and is given by (15). The F_{min} calculated from (15) was compared with F_{min} measured at 1.5 GHz and was found to be within the range of measurement uncertainty.

Given the three parameters R_n, G_{in}, and G_c, the value of F_{min} for the device can be calculated at any desired frequency and dc bias from (13). Calculated values of F_{min} are plotted in Fig. 8 (a) and (b), as a function of I_D and f_o, respectively. There was no variation with V_{DS} over the normal voltage range. In addition, F_{min} was measured for the same devices mounted on a carrier, in a conventional microwave noise figure measurement setup employing a commercial automatic noise figure meter, and the results of these measurements are also included in Fig. 8 (a) and

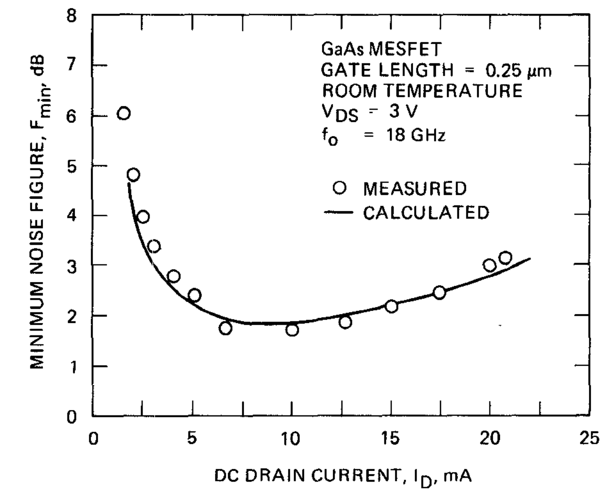

(a)

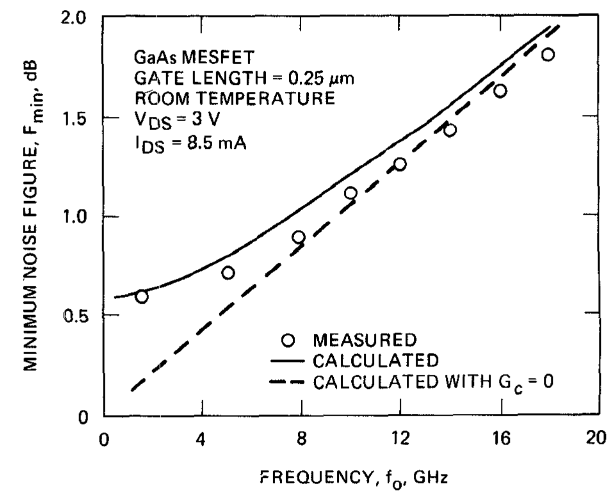

(b)

Fig. 8. Comparison of the calculated and measured values of the MESFET minimum noise figure F_{min} at room temperature. (a) Dependence of F_{min} on dc drain current I_D at $f_o = 18$ GHz. (b) Dependence of F_{min} on operating frequency f_o at $I_D = 8.5$ mA.

(b). The good agreement over a range of dc bias and frequency verifies the utility of the noise model, as well as the assumptions made in Section II-E.

B. Comparison with Podell's Empirical Model

The only other model available in the literature having the simplicity of the above model is the one described by Podell [8]. The present work differs from the empirical model of Podell in several ways:

(i) In Podell's model, the input and output noise current sources i_{in} and i_o are required to be uncorrelated. The analysis of the present paper remains valid even if the correlation between the two sources is high, since only the real part, rather than the magnitude, of the correlation coefficient has been assumed to be small. Theoretical models of MESFET noise do indeed show that the correlation coefficient between i_{in} and i_o is large and purely imaginary [4].

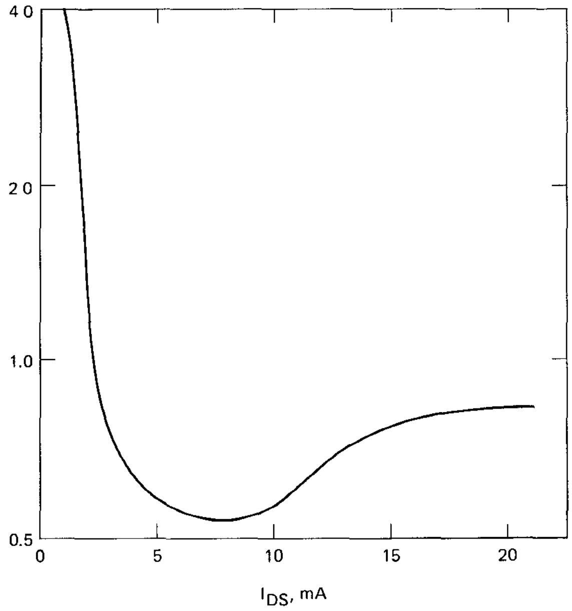

Fig. 9. Podell's empirical constant Q, calculated from measured values of device transconductance g_m and output noise current spectral density S_{id} at 1 GHz.

(ii) No circuit model or losses are included in Podell's model; as a result, the relationships in [8] can be recovered from the results of Section II by setting G_c at zero. This leads Podell to the conclusion that a single measurement of $F_{\min}$ at any frequency, along with the small-signal equivalent circuit model of the MESFET, can be used to determine $F_{\min}$ at any other frequency. Our model shows that the calculation of $F_{\min}$ requires a knowledge of the two parameters S_{io} and G_c in addition to the small-signal equivalent circuit model of the MESFET. If G_c is set equal to zero, the calculated values of $F_{\min}$ are lower, as indicated by the dashed curve in Fig. 8(b), and the error becomes increasingly larger at lower frequencies.

(iii) The output noise current is characterized in Podell's model by an equivalent noise resistance R_n, and its bias dependence is given by the empirical relationship

$$Q \equiv g_m R_n = K_0 \exp(K_2 I_D / I_{DSS}) \tag{20}$$

where K_0 and K_2 are empirical factors. Our measurements show that the empirical relationship (20) does not apply to the devices under test. The measured values of the quantity Q in (20) are plotted in Fig. 9 as a function of I_D. It is apparent that the plot is not described by the functional relationship in (20), particularly in the low-noise range of bias currents, where the device is most likely to be operated.

V. Summary and Significance of Results

This paper has established a procedure whereby the minimum noise figure of a MESFET can be predicted at microwave frequencies solely from on-wafer measurements. The advantages of this method compared with the actual microwave measurement of $F_{\min}$ include the following:

(i) No individual tuning of devices is required for identifying the minimum of the noise figure.

(ii) Measurements are simpler, faster, and less subject to the uncertainty whether a minimum value of F has indeed been reached.

(iii) Measurements can be performed at the wafer stage of device fabrication, prior to device dicing, mounting, bonding, etc.

(iv) Measurement is possible on production batches, using automated test equipment.

(v) Unlike the measurement of a single quantity such as $F_{\min}$, which does not reveal the cause of a very high or low value of $F_{\min}$, the measurement method presented here isolates the cause of an abnormal $F_{\min}$ value among the several contributing factors. The measurement is therefore useful for diagnostic work during device development.

A figure of merit for MESFET's may also be deduced from the results of this paper. In low-loss circuits, the inherent $F_{\min}$ of the device is given by (17). This is a monotonic function of the product $R_n G_{in}$. Therefore the inverse of this product can serve as a measure of the low noise capability of the device, and it has a simple physical interpretation: for very low noise devices in which $R_n G_{in}$ is very small, (17) can be approximated as

$$F_{\min} = 1 + 2\sqrt{R_n G_{in}} \tag{21}$$

from which it follows that

$$1/R_n G_{in} = 2/(F_{\min} - 1)^2. \tag{22}$$

The quantity $1/R_n G_{in}$ has the advantage that it is dimensionless; it is, however, a function of frequency.

A figure of merit dependent only on device parameters and independent of frequency can also be defined. At moderate frequencies, defined by (10), the above measure of low-noise capability is proportional to the quantity $g_m^2/S_{io}C_{gs}^2R_T$, which can serve as a figure of merit for comparing devices with each other.

Acknowledgment

The authors thank Dr. C. F. Krumm and Dr. R. E. Lee for the management of the research program which led to this work, and for their encouragement and guidance. The authors also thank J. Marzan for the design and fabrication of probes used for on-wafer measurement, as well as test fixtures for the characterization of diced and mounted MESFET's.

References

[1] M. W. Pospieszalski, "X-band noise performance of commercially available GaAs FETs at room and cryogenic temperatures," Tech. Rep. No. 260, Electronics Division, National Radio Astronomy Observatory, Charlottesville, VA, 1986.

[2] R. Q. Lane, "Derive noise and gain parameters in 10 seconds," *Microwaves*, vol. 17, no. 8, pp. 53–57, Aug 1978.

[3] R. Froelich, "Measurement of GaAs FET noise parameters," *Watkins Johnson Co. Tech-Notes*, vol. 13, no. 6, pp. 2–11, Nov./Dec. 1986

[4] H. Statz, H. A. Haus, and R. A. Pucel, "Noise characteristics of gallium arsenide field-effect transistors," *IEEE Trans Electron Devices*, vol. ED-21, pp. 549–562, Sept. 1974.

[5] B. Carnez, A. Cappy, R. Fauquembergue, E. Constant, and G. Salmer, "Noise modeling in submicrometer-gate FET's," *IEEE Trans. Electron Devices*, vol. ED-28, pp. 784–789, July 1981.

[6] H. Fukui, "Optimal noise figure of microwave GaAs MESFET's," *IEEE Trans. Electron Devices*, vol. ED-26, pp. 1032–1037, July 1979.

[7] C. H. Oxley and A. J. Holden, "Modified Fukui model for high-frequency MESFETs" *Electron. Lett.*, vol. 22, no. 13, pp. 690–692, June 19, 1986.

[8] A. F. Podell, "A functional GaAs FET noise model," *IEEE Trans. Electron Devices*, vol. ED-28, pp. 511–517, May 1981.

[9] M. K. Ahmed, "Empirical determination of the noise figure of GaAs MESFETs," *Frequenz*, vol. 38, no. 12, pp. 313–317, Dec. 1984.

[10] H. Fukui, Ed., *Low-Noise Microwave Transistors and Amplifiers*. New York: IEEE Press, 1982.

[11] S. Weinreb, "Low noise cooled GASFET amplifiers," *IEEE Trans. Microwave Theory Tech.*, vol. MTT-28, pp. 1041–1054, Oct. 1980.

[12] H. Rothe and W. Dahlke, "Theory of noisy fourpoles," *Proc. IRE*, vol. 44, no. 6, pp. 811–818, June 1956.

[13] K. Ohata, H. Itoh, F. Hasegawa, and Y. Fujiki, "Super low-noise GaAs MESFET's with a deep-recess structure," *IEEE Trans. Electron Devices*, vol. ED-27, pp. 1029–1034, June 1980.

[14] M. S. Gupta, "Detection of avalanching in submicron gate length MESFET's," *IEEE Electron Device Lett.*, vol. EDL-8, pp. 469–471, Oct. 1987.

[15] M. S. Gupta and P. T. Greiling, "Microwave noise characterization of GaAs MESFETs—II: Determination of extrinsic noise parameters," *IEEE Trans. Microwave Theory Tech.*, to be published.

[16] D. B. Estreich, "A wideband monolithic GaAs IC amplifier," in *1982 Int. Solid-State Circuits Conf. Dig.* (San Francisco, CA), Feb. 1982, pp. 194–195, 318.

[17] IRE Subcommittee 7.9 on Noise (H. A. Haus, Chairman), "IRE standards on methods of measuring noise in linear twoports, 1959," *Proc. IRE*, vol. 48, no. 1, pp. 60–68, Jan. 1960.

[18] W. C. Bruncke and A. van der Ziel, "Thermal noise in junction-gate field-effect transistors," *IEEE Trans. Electron Devices*, vol. ED-13, pp. 323–329, Mar. 1966.

[19] K. E. Jones, E. W. Strid, and K. R. Gleason, "mm-wave wafer probes span 0 to 50 GHz," *Microwave J.*, vol. 30, no. 4, pp. 177–183, Apr. 1987.

[20] M. S. Gupta, "Noise in oscillators employing submicron field-effect transistors," in *Proc. 41st Ann. Frequency Control Symp.* (Philadelphia, PA), May 1987.

[21] M. S. Gupta, "Bias dependence of diffusion noise in GaAs MESFETs with submicron gate lengths," in *Proc. 9th Int. Conf. Noise in Physical Systems*, (Montreal, Canada), May 1987.

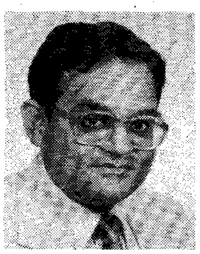

Madhu S. Gupta (S'68–M'72–SM'78) received the master's and Ph.D. degrees in 1968 and 1972, respectively, from the University of Michigan, Ann Arbor.

While at the University of Michigan, he was a member of the Electron Physics Laboratory, and carried out research on the large-signal and noise characteristics of microwave semiconductor devices. During 1973–79, he was first an Assistant Professor and then an Associate Professor of Electrical Engineering at the Massachusetts Institute of Technology, Cambridge, where he was a member of the M.I.T. Research Laboratory of Electronics, and conducted research on microwave and millimeter-wave semiconductor devices, related high-field transport properties, and thermal fluctuations. Since 1979, he has been at the University of Illinois at Chicago, where he is presently a Professor of Electrical Engineering, and works on the materials, design, characteristics, limitations, and noise of high-frequency, nonlinear, active, and/or very small electron devices. During 1985–86, he was a Visiting Professor at the University of California, Santa Barbara.

Dr. Gupta is a member of Eta Kappa Nu, Sigma Xi, and Phi Kappa Phi. He is a registered Professional Engineer, and has served as the chairman of the Boston and Chicago chapters of the IEEE Microwave Theory and Techniques Society. He is the editor of *Electrical Noise: Fundamentals and Sources* (IEEE Press, 1977), *Noise in Circuits and Systems* (IEEE Press, 1987), and *Teaching Engineering: A Beginner's Guide* (IEEE Press, 1987), and was the recipient of a Lilly Foundation Fellowship.

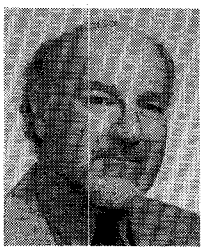

Octavius Pitzalis, Jr. (S'58–M'60) is presently senior staff scientist at EEsof, Inc., Westlake Village, CA. He received the B.S.E.E. degree from the University of Missouri at Columbia in 1959 and did graduate studies at New York University from 1963 to 1966.

From 1978 to 1987 he was a member of the technical staff at Hughes Research Laboratories–Malibu, where he was responsible for MMIC design, FET modeling and characterization, and the development of microwave power combiners for FET's and IMPATT diodes. From 1959 to 1978 Mr. Pitzalis was a research engineer at the U.S. Army Research and Development Command at Fort Monmouth, NJ, where he was involved in the earliest micropower transistor analog and logic circuit design for silicon integrated circuits, and in developing broad-band circuit design techniques for microwave transistor power amplifiers.

Steven E. Rosenbaum (M'87) received the B.S.E.E. degree from the University of Michigan in 1983. He is currently a Hughes Aircraft Fellow and is working toward the M.S. degree in electrical engineering at the University of California, Los Angeles.

Since joining Hughes in 1983, Mr. Rosenbaum has been involved in the design of several conventional and monolithic microwave and millimeter-wave circuits. He has also worked extensively in the development of highly accurate microwave measurement techniques for devices and circuits. At the Research Laboratories, he has primarily focused on the measurement and modeling of GaAs MESFET's and HEMT's at millimeter-wave frequencies.

Paul T. Greiling (S'64–SM'82–F'85) received the B.S.E.E. and B.S. Math. degrees in 1963, the M.S.E.E. degree in 1964, and the Ph.D. degree in 1970, all from the University of Michigan, Ann Arbor.

He joined the Department of Electrical Engineering at Northeastern University, Boston, MA, in 1970. While at Northeastern, he consulted for the M.I.T. Lincoln Laboratory in the area of IMPATT diodes. In 1972, he joined the faculty of Electrical Sciences and Engineering at the University of California, Los Angeles, where he did research on the theoretical analysis and experimental characterization of microwave solid-state devices. He consulted for local industry on millimeter-wave semiconductor devices. In 1976 he was a Visiting Faculty Member at Sandia Laboratory, Albuquerque, NM, working on GaAs FET's. In 1976, he joined the staff at Hughes Research Laboratories, Malibu, CA, where he has been responsible for the design, modeling, and testing of GaAs digital IC's.

Dr. Greiling was selected as a Distinguished Microwave Lecturer by the MTT-S for 1984–1985 and presented a lecture on "High-Speed Digital IC Performance Outlook" to MTT chapters throughout the US, Europe, and Japan. At present, he is Manager of the GaAs Devices and Circuits Department at Hughes Research Laboratories working on high-speed GaAs logic circuits and is an Adjunct Professor in the Electrical Sciences and Engineering Department at UCLA. Dr. Greiling is a member of MTT-S AdCom, Eta Kappa Nu, Tau Beta Pi, and Sigma Xi.